

# Excimer Laser Induced Bubble: Dimensions, Theory, and Implications for Laser Angioplasty

Ton G. van Leeuwen, PhD, E. Duco Jansen, PhD, Ashley J. Welch, PhD, and  
Cornelius Borst, MD, PhD

Department of Cardiology, Heart Lung Institute, Utrecht University Hospital, Utrecht,  
The Netherlands

**Background and Objective:** Previous studies have demonstrated that during Xenon-Chloride excimer laser ablation of tissue, rapidly expanding and imploding bubbles (diameter < 3 mm), predominantly containing water vapor, are formed. These short lived bubbles (life time < 300  $\mu$ s) induce mechanical damage in adjacent tissue. In the present study, a theoretical analysis of the volume of vaporized water is correlated with measured bubble volumes formed in hemoglobin solution.

**Study Design/Materials and Methods:** The dimensions of the rapidly expanding and imploding vapor bubble induced by the XeCl excimer laser pulses (308 nm, 115 ns), delivered via a 300, 550, or 950  $\mu$ m diameter monofiber in 16% w/v hemoglobin solution (at 37°C), were measured.

**Results:** Theoretical analysis and the experimental data correlated well (correlation coefficient  $r = 0.97$ ). The diameter of excimer laser induced bubbles increased with increasing pulse energy. For a given radiant exposure, the bubble size was decreased by either decreasing the fiber tip area or by decreasing the absorption coefficient of the hemoglobin solution.

**Conclusion:** We conclude that, for a wide range of conditions, theory agrees well with experimental data. Thus, during delivery of excimer laser pulses in blood, bubble dimensions can be reduced by flushing with saline or by reduction of the area radiated with each laser pulse, for example, by pulse multiplexing or using a smaller multifiber catheter. © 1996 Wiley-Liss, Inc.

**Key words:** Xenon-Chloride excimer laser, pulsed laser, vaporization, cavitation, blood

## INTRODUCTION

Ultra-violet xenon-chloride excimer laser light (wavelength  $\lambda = 308$  nm, pulse length up to 220 ns) is strongly absorbed by proteins, lipids, and nucleic acids [1]. Consequently, its penetration depth,  $\delta$ , is very small in aortic tissue ( $\delta \approx 100$   $\mu$ m) [2] as well as in blood ( $\delta \approx 30$   $\mu$ m) [3,4]. Although excimer laser light is not absorbed by water [5], recent in vitro and in vivo studies have demonstrated that excimer laser pulses create water vapor bubbles, that rapidly expand and collapse [6–8], both in tissue [9] and in blood [3]. It has been hypothesized that the absorbed energy is transferred to surrounding (tissue) water [10],

which subsequently vaporizes explosively. In previous in vivo experiments [3,9], we demonstrated that the rapidly expanding and imploding vapor

Accepted for publication February 3, 1995.

Address reprint requests to Ton G. van Leeuwen, Ph.D., Experimental Cardiology Laboratory, Utrecht University Hospital, Room G02.523, P.O. Box 85500, 3508 GA Utrecht, The Netherlands.

Ton G. van Leeuwen is at Interuniversity Cardiology Institute of the Netherlands, Utrecht, The Netherlands.

E. Duco Jansen and Ashley J. Welch are in the Biomedical Engineering Program, University of Texas, Austin, Texas.

bubble (lifetime 50 to 300  $\mu\text{s}$ , diameter up to 3 mm) creates dissections, whose extent (over 1 mm) exceeds the penetration depth of the laser light in tissue.

To reduce the bubble dimensions and to consequently reduce the mechanical damage, two new laser light delivery strategies have been proposed recently. One strategy is based on flushing with saline during the laser angioplasty procedure [11], which results in a lower absorption coefficient of the diluted blood. The other strategy is based on dividing the energy (but not the radiant exposure) of one excimer laser pulse (both spatially and in time) in eight to 12 smaller excimer laser pulses ("multiplexing") [12]. Although both strategies are clinically applied, up to now neither theoretical nor experimental data on the bubble reduction is available.

The aim of this study was to quantify the dimensions of the excimer laser induced vapor bubbles in a hemoglobin solution with an absorption coefficient similar to that of blood. A relation between the volume of the induced vapor bubble and laser-tissue parameters such as the energy of the delivered laser pulse, the ablative surface area of the fiber tip, and the absorption coefficient of the medium is correlated with experimental data. The relation is based on the results of our previous studies [13,14] in which we concluded that the excimer-induced short-lived vapor bubble derives predominantly from vaporized water.

## THEORY

The threshold energy for bubble formation in water is only determined by the energy needed to reach a temperature of 100°C [13]. In other words, the threshold energy requirements for bubble formation are limited to the requirements to form water vapor at nucleation sites and not to the amount of energy to vaporize water across the entire area of the delivery fiber. As a result, assuming Beer's law of laser light attenuation in the target liquid and assuming no heat losses and no changes in absorption coefficient during the laser pulse, the (theoretical) threshold radiant exposure,  $H_{th}$ , for bubble formation is given by the radiant exposure that induces the boiling temperature of water (see Appendix):

$$H_{th} = \frac{\rho c \Delta T}{\mu_a} \left[ \frac{mJ}{mm^2} \right] \quad (1)$$

where  $\rho$  is the density of water [1 mg/mm<sup>3</sup>],  $c$  is the specific heat of water [4.2 mJ/mg °C],  $\Delta T$  is the difference between the boiling temperature of water and the ambient water temperature [°C] and  $\mu_a$  is the absorption coefficient for the laser light [mm<sup>-1</sup>]. Consequently, the infinitesimally thin disc in front of the fiber tip is only *partially vaporized*, which is described by a factor  $f \leq 1$ , the fraction of the area that is vaporized. The fraction of the vaporized surface area  $f(x)$  depends on the absorbed energy at depth  $x$  (Beer's law). Integrating this fraction  $f(x)$  from the fiber tip ( $x = 0$ ,  $H = H_0$ ) to the depth  $d$  at which  $H(d) = H_{th}$  gives the maximal volume of water,  $V_{liq}$ , beneath the fiber tip that can be vaporized by a laser pulse with radiant exposure  $H_0$  for  $H_{th} < H_0 < 9.5H_{th}$  (see Appendix):

$$V_{liq} = \frac{AH_{th}}{\rho L_v} \left( \frac{H_0}{H_{th}} - 1 - \ln \left( \frac{H_0}{H_{th}} \right) \right) [mm^3] \quad (2)$$

where  $L_v$  is the latent heat of vaporization of water [2260 mJ/mg] and  $A$  is the surface area of the fiber tip [mm<sup>2</sup>].

Thus, for a given ratio of  $H_0/H_{th}$  ( $1 < H_0/H_{th} < 9.5$ ), the volume of vaporized water is proportional to the surface area  $A$  of the fiber tip. The ratio of volume  $V_{liq}$  and the surface area  $A$  of the fiber tip depends on  $H_0$  and  $H_{th}$  only.

$$\frac{V_{liq}}{A} = \frac{H_{th}}{\rho L_v} \left( \frac{H_0}{H_{th}} - 1 - \ln \left( \frac{H_0}{H_{th}} \right) \right) [mm] \quad (3)$$

As  $H_{th}$  depends on the absorption coefficient  $\mu_a$  (eq. 1), the following relation between volume  $V_{liq}$  and absorption coefficient can be derived (combining Eqs. 1 and 2):

$$V_{liq} = \frac{A}{\rho L_v} \left( H_0 - \left( \frac{\rho c \Delta T}{\mu_a} \right) \left( 1 + \ln \left( \frac{H_0 \mu_a}{\rho c \Delta T} \right) \right) \right) [mm^3] \quad (4)$$

The volume of vaporized water  $V_{liq}$  will expand to a much larger volume of water vapor. The ratio of the maximal volume of the water vapor bubble  $V_{vap}$  to the volume of the vaporized water  $V_{liq}$  depends on the pressure of the bubble at maximal dimensions, the rate of condensation during expansion, and possible catheter-induced boundary effects. Assuming that:

$$V_{\text{vapor}} = \Omega V_{\text{liq}} \quad [\text{mm}^3] \quad (5)$$

where  $\Omega$  is the volume expansion coefficient, then the volume of the vapor bubble is given by:

$$V_{\text{vapor}} = \Omega \frac{AH_{\text{th}}}{\rho L_v} \left( \frac{H_0}{H_{\text{th}}} - 1 - \ln \left( \frac{H_0}{H_{\text{th}}} \right) \right) \quad [\text{mm}^3] \quad (6)$$

## MATERIALS AND METHODS

### Fibers and Absorbing Media

To determine the relation between vapor bubble volume and radiant exposure, excimer laser pulses were delivered via 300, 550, and 950  $\mu\text{m}$  diameter bare fibers in stroma-free human hemoglobin (16% weight/volume) in phosphate buffered saline solution. The absorption coefficient of the hemoglobin solution at 308 nm was  $32.1 \pm 0.6 \text{ mm}^{-1}$  (mean  $\pm$  standard deviation,  $n = 6$ , measured by a spectrophotometer) [3] and its temperature was maintained at  $37^\circ\text{C}$  throughout the experiment. Thus, the theoretical threshold radiant exposure for bubble formation was  $8.2 \pm 0.2 \text{ mJ/mm}^2$ , using equation 1 and the thermal properties of water. The delivered energy ranged from 1.25 to 51  $\text{mJ/pulse}$  (9 to 80  $\text{mJ/mm}^2$ ) and the ratio of radiant exposure to theoretical threshold radiant exposure ( $H_0/H_{\text{th}}$ ) ranged up to 9.5. Using equation 6, the ratio of theoretically calculated vaporized water volume to the surface of the fiber top (eq. 3) was correlated with the ratio of measured bubble volume to the surface area of the fiber tip.

Using equation 5, the relation between the vaporized volume liquid water as a function of absorption coefficient (eq. 4) and the measured bubble volume was determined. XeCl excimer laser pulses (50–55  $\text{mJ/mm}^2$ ) were delivered via a bare fiber (300, 550, or 950  $\mu\text{m}$  diameter) in hemoglobin solutions of different concentrations (2 to 16% w/v), resulting in absorption coefficients ranging from 4 to 32  $\text{mm}^{-1}$  for 308 nm light [3].

### Data Analysis

The maximal diameter perpendicular to the fiber axis (width), the maximal diameter coaxial with the fiber (height) and the lifetime of XeCl excimer laser ( $\lambda = 308 \text{ nm}$ ,  $\tau_p = 115 \text{ ns}$ ) induced bubbles were measured by time-resolved flash photography [15]. From the measured width and height, the maximal volume was determined, assuming an ellipsoidal vapor bubble and taking

into account the volume occupied by the fiber tip within the bubble. The measured volume  $V_{\text{vapor}}$  was approximated by:

$$V_{\text{vapor}} = \pi \left( \frac{w^2 h}{6} - \frac{\Phi^2}{4} \left( h - \frac{w}{2} \right) \right) \quad [\text{mm}^3] \quad (7)$$

with  $w$  and  $h$  the measured width and height of the vapor bubble, respectively, and  $\phi$  the diameter of the fiber or catheter. Each data point was the average bubble volume ( $\pm$  sd) of eight measurements. The lifetime of the bubble was defined as the time between onset of bubble formation and point of first collapse.

Experimentally obtained data were compared to the described partial vaporization hypothesis by correlating the measured volume of the bubble  $V_{\text{vapor}}$  with the calculated vaporized volume  $V_{\text{liq}}$  (eq. 2). Using all data points and equation 5, the expansion factor  $\Omega$  (ratio of  $V_{\text{vap}}$  to  $V_{\text{liq}}$ ) was determined using the least squares method.

## RESULTS

The excimer induced vapor bubbles were elliptically shaped: their maximal width was larger than their height. The maximal width, height, and volume of the bubble increased with increasing energy and increasing absorption coefficient. Thus, for a constant radiant exposure of 50–55  $\text{mJ/mm}^2$ , the bubble size decreases with decreasing delivered energy and with decreasing hemoglobin concentration (Fig. 1).

In Figure 2, the measured diameters (widths) of the excimer laser induced bubbles in hemoglobin solution (16% w/v) are plotted. Note that by decreasing the ablative surface area of the fiber at a constant radiant exposure, the maximal bubble diameter decreased (Fig. 2A). From Figure 2B, it is clear that the delivered energy per pulse is not the only parameter which determines the maximal dimensions of the short-lived vapor bubble. In Figure 3, it is shown that a high correlation ( $R = 0.98$ ) existed between the lifetime of the bubble and the maximal diameter (width).

### Theory Versus Measurements

For all data taken together, a high correlation ( $R = 0.97$ ) between theoretical volume of vaporized liquid water (eq. 3) and measured bubble volume was established when the volume expansion coefficient  $\Omega$  was fitted to be 4,400. For the

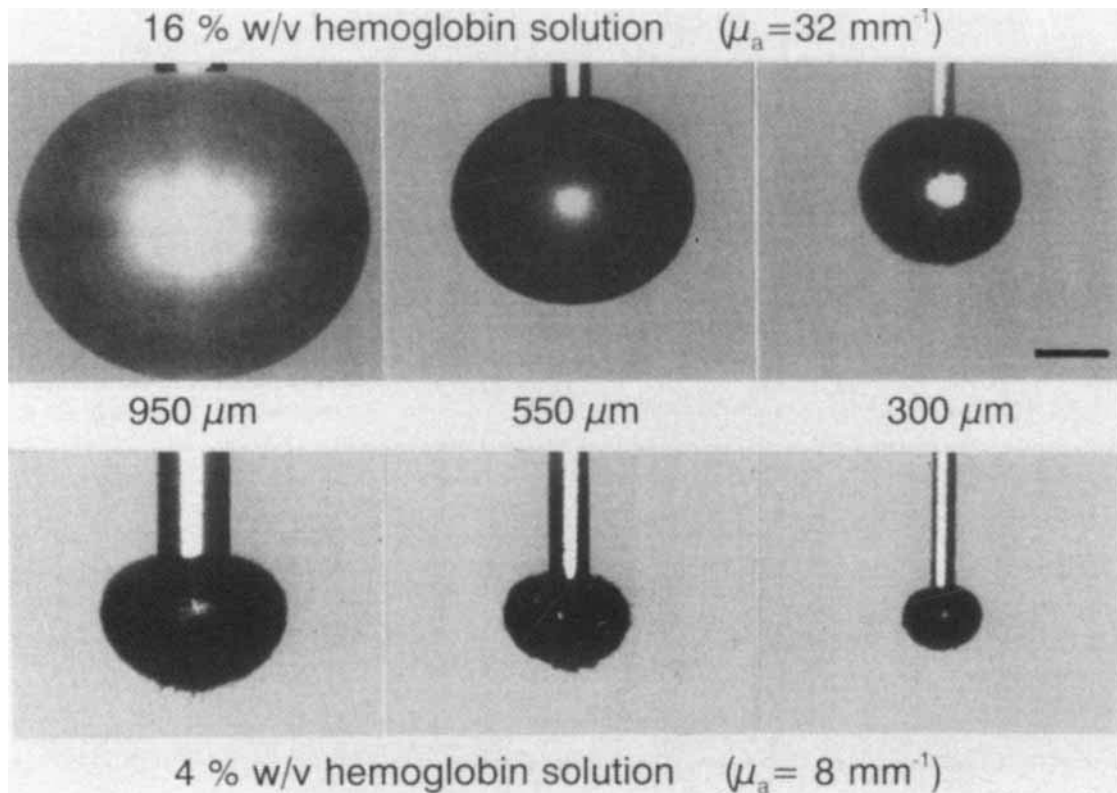


Fig. 1. Compilation of time resolved photographs of excimer laser induced bubbles in 16% (w/v) hemoglobin solution (top panel) and 4% (w/v) hemoglobin solution (bottom panel). The left, middle, and right bubbles are induced by excimer laser

pulses (at a radiant exposure of 50–55 mJ/mm<sup>2</sup>) delivered via a 950  $\mu$ m, 550  $\mu$ m, and 300  $\mu$ m diameter monofiber, respectively.

undiluted hemoglobin solution, the ratio of bubble volume and surface area of the monofiber tips ( $V/A$ ) as a function of the ratio of radiant exposure over theoretical threshold radiant exposure ( $H_0/H_{th}$ ) is plotted in Figure 4.

Diluting the hemoglobin solution with saline resulted in a decreased absorption coefficient. Consequently, the measured bubble diameter (width) decreased (Fig. 5). Note again that the measured width as a function of the absorption coefficient correlated well with the theory (eqs. 4 and 5,  $\Omega$  is 4,400).

## DISCUSSION

The aim of this study was to determine the dimensions of rapidly expanding and imploding vapor bubbles induced by 308 nm excimer laser pulses delivered in a hemoglobin solution. The principal finding of this study was that a high correlation was found between the maximal volume of the vapor bubble and the delivered energy, fiber tip area and the absorption coefficient of the

medium. These parameters were implemented in a simple model.

## Theory Versus Measurements

The absorption coefficient of the hemoglobin solution (Fig. 5) was varied from 4 to 32 mm<sup>-1</sup> (a factor 8) and the surface area of the fiber tip (Fig. 4) was varied from 0.071–0.71 mm<sup>2</sup> (a factor 10). Also, the delivered energy per pulse ranged from 1.25 to 51 mJ. Thus, although the range of the different parameters was large, still the correlation between theory and measurements was high ( $R = 0.97$ ), indicating the usefulness of the model for predicting the bubble dimensions.

The *partial vaporization theory* [14] is based on (see appendix) vaporization of water in the hemoglobin solution at nucleation sites which reached a temperature of 100°C. Furthermore, it was assumed that the ratio of the resulting volume of vapor and the vaporized liquid water volume (the factor  $\Omega$ ) is independent on the delivered energy, laser pulse length, the surface area of the

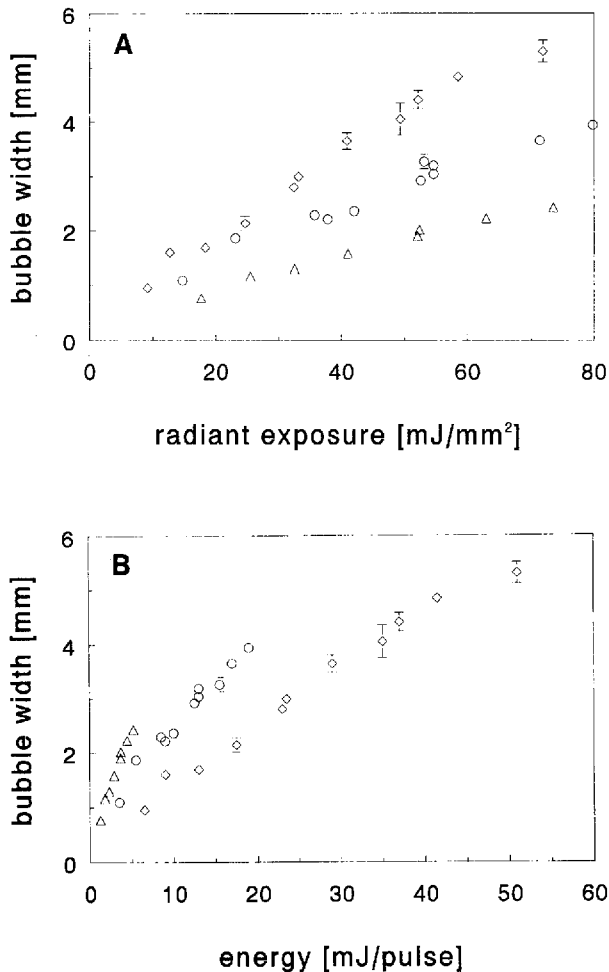


Fig. 2. The measured maximal width of the excimer laser induced vapor bubbles in hemoglobin solution ( $\mu_a = 32 \text{ mm}^{-1}$ ) at 37°C as a function of (A) the radiant exposure, and (B) energy per pulse.  $\Delta$ : fiber diameter  $\phi = 300 \mu\text{m}$ ;  $\circ$ :  $\phi = 550 \mu\text{m}$ ;  $\diamond$ :  $\phi = 950 \mu\text{m}$ . Data points are presented as mean ( $\pm$  sd, if sd is larger than the symbol,  $n = 8$ ).

fiber tip, and the absorption coefficient of the medium.

The assumption that the volume expansion factor  $\Omega$  is constant is commonly made for boiling water. At the boiling point, the absorbed energy is used for volume expansion due to the conversion of liquid water to water vapor. The temperature is supposed to be constant, thus the specific volume, which depends directly on the temperature of the vapor, will be constant. At 1 bar, the ratio of the specific volume of water vapor at 100°C [ $1.674 \text{ m}^3/\text{kg}$ ] to the specific volume of liquid water at 37°C [ $1.007 \cdot 10^{-3} \text{ m}^3/\text{kg}$ ] is 1,662 [16]. In the present study, the fitted volume expansion factor  $\Omega$  is larger than 1,662, suggesting that the pressure inside the bubble at maximal expansion is

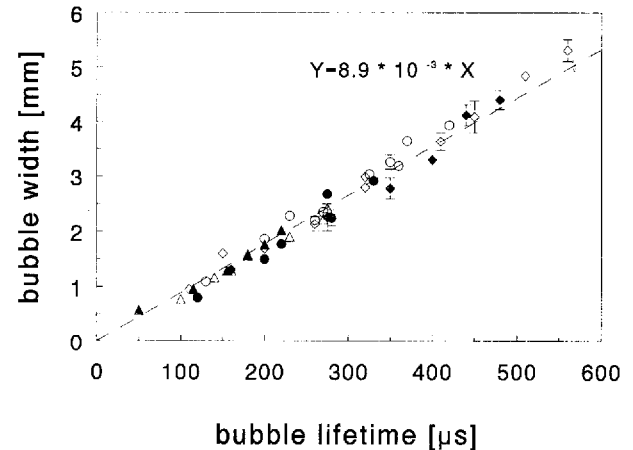


Fig. 3. The measured maximal width of the excimer laser induced vapor bubbles in hemoglobin solution at 37°C as a function of the measured lifetime of the bubble. Open symbols:  $\mu_a = 32 \text{ mm}^{-1}$  and the radiant exposure was varied; filled symbols: radiant exposure was constant ( $50\text{--}55 \text{ mJ/mm}^2$ ) and  $\mu_a$  varied from 4 to  $32 \text{ mm}^{-1}$ .  $\Delta$ : fiber diameter  $\phi = 300 \mu\text{m}$ ;  $\circ$ :  $\phi = 550 \mu\text{m}$ ;  $\diamond$ :  $\phi = 950 \mu\text{m}$ . Data points are presented as mean ( $\pm$  sd, if sd is larger than the symbol,  $n = 8$ ). Interrupted line is the least squares fit through the origin ( $R = 0.98$ ).

smaller than 1 bar. Thus the maximal bubble volume is also determined by the dynamics of the preceding expansion phase. Then, during the expansion phase, the surface tension of the bubble water interface decreases, whereas the inertia of the moving liquid increases [17]. These effects depend on the initial dimension of the vaporized water. Also, the shape of the smaller bubbles is more eccentric. As a result, the volume expansion factor  $\Omega$  may not be independent of the initial volume of vaporized water. Then, the volume expansion factor  $\Omega$  depends on the radiant exposure. In Figure 4, two additional curves have been drawn using equation 6 with volume expansion factors  $\Omega$  of 3,400 and 5,400, suggesting a possible dependence of  $\Omega$  on radiant exposure. A volume expansion factor  $\Omega$  of 3,400 seems to be better for smaller bubbles, whereas a volume expansion factor  $\Omega$  of 5,400 may be a better parameter for the larger bubble volumes.

The threshold radiant exposure for this article was based on equation 1 using the thermal properties of water at 1 bar. In practice, the experimental threshold radiant exposure may be or seem to be lower due to impurities in the absorbing medium or by non-flat (top-hat or gaussian) beam profiles [18]. Furthermore, we assumed that  $\rho_c$  of the hemoglobin solutions was similar to that of water. All these parameters are hard to deter-

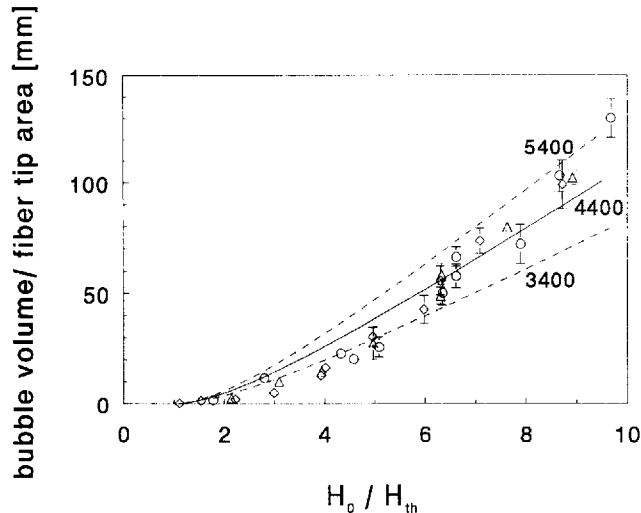


Fig. 4. Ratio of maximal bubble volume  $V$  to surface area  $A$  of the monofiber catheter as a function of the ratio of radiant exposure  $H_0$  to theoretical threshold radiant exposure  $H_{th}$  for bubble formation in hemoglobin solution at 37°C.  $H_{th} = 8.2$  mJ/mm<sup>2</sup>,  $\mu_a = 32$  mm<sup>-1</sup>. The solid line is a least squares curve fit according to equation 5, with  $V_{liq}$ /surface area  $A$  of the fiber tip calculated by equation 3 and the volume expansion coefficient  $\Omega$  fitted to be 4,400 (correlation coefficient  $R = 0.97$ ).  $\Delta$ : diameter  $\phi = 300$   $\mu$ m;  $\circ$ :  $\phi = 550$   $\mu$ m; and  $\diamond$ :  $\phi = 950$   $\mu$ m monofiber. The dotted lines represent curves given by equation 6 where  $\Omega$  is 3,400 and 5,400.

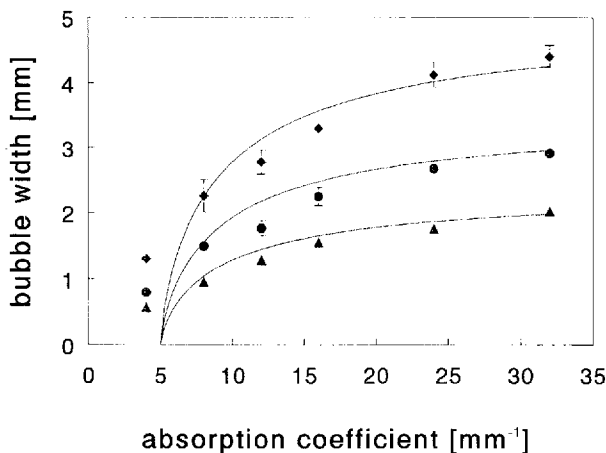


Fig. 5. The maximal width of excimer laser induced vapor bubbles in hemoglobin solution (at 37°C) as a function of the absorption coefficient.  $\Delta$ : fiber diameter  $\phi = 300$   $\mu$ m;  $\bullet$ :  $\phi = 550$   $\mu$ m;  $\blacklozenge$ :  $\phi = 950$   $\mu$ m. The radiant exposure was 50–55 mJ/mm<sup>2</sup>. The lines are the least squares curve fits of equation 5, using all data points and the volume expansion coefficient  $\Omega = 4,400$  ( $R = 0.97$ ). Data points are presented as mean ( $\pm$  sd, if sd is larger than the symbol,  $n = 8$ ).

mine, and therefore we used 100°C as the threshold temperature for water vapor formation. Thus, the only fitted parameter was the volume expansion factor  $\Omega$ .

## Clinical Implications

We have demonstrated that the rapidly expanding and imploding vapor bubble induced by an ablative excimer laser pulse causes dissections [3,9]. At this moment, two strategies (multiplexing and saline flushing) to reduce the bubble dimensions (and thus to reduce its collateral damage) are clinically used. Multiplexing a laser pulse (at a given radiant exposure) results in a number (8–12) of smaller laser pulses (with the same given radiant exposure) delivered consecutively at different sectors of the multifiber catheter. From equation 6 it is derived that, at constant radiant exposure, the bubble volume is proportional to the ablative area of the catheter tip. The diameter of the bubble is proportional to the root cubed of the bubble volume, thus the bubble diameter is also proportional to the root cubed of the ablative area of the catheter. Thus, to decrease the bubble diameter by a factor of 2, the ablative area of the catheter has to be decreased by a factor of 8.

Decreasing the bubble volume by dilution of the blood by providing a saline flush during laser angioplasty procedures is an alternative approach. From Figure 5 it is derived from the partial vaporization model and the experimental data, that, at a constant radiant exposure of 50–55 mJ/mm<sup>2</sup>, to decrease the bubble diameter by a factor of 2 (volume by a factor of 8), the absorption coefficient has to be decreased from 32 mm<sup>-1</sup> by a factor of 4.0 to 8 mm<sup>-1</sup>. However, note that saline flushing only decreases the bubble size induced in blood, whereas the multiplexing is expected to reduce the dimension of the bubble induced in and on the target tissue.

The lifetime of the bubble is proportional to its maximal diameter (width, Fig. 3). In 1917, Lord Rayleigh predicted this linear relation for “empty” cavitation bubbles [17]. The relation between the diameter and lifetime of the vapor bubble may be useful for measuring the diameter of excimer laser induced vapor bubbles in blood. Due to the scattering by the red blood cells, time-resolved flash photography is not appropriate. Then, the lifetime of the bubble can be measured by optical probing by a helium-neon laser [19] or by an acoustic transducer [20]. At the moment of bubble formation and at the moment of bubble collapse an acoustic transient, which is not necessarily a shock-wave, is generated. The time difference between the acoustic transients is the lifetime of the bubble. In both ways, it might even be

possible to measure the bubble dimension in vivo and therefore serve as a feedback control.

At present, for laser angioplasty, multifiber catheters are used. The first generation multifiber catheters consisted of approximately 12–20 fibers of 100  $\mu\text{m}$  diameter, resulting in an active irradiation area of approximately 10% of the catheter tip. The poor results of excimer laser angioplasty were blamed on the large, dead space, which during recanalization, necessitated a mechanical dotter effect of the catheter [11,21]. Nowadays, multifiber catheters consist of 100–200 fibers of 50  $\mu\text{m}$  diameter each, resulting in an active irradiation area of up to 24% of the catheter tip. As a result, for a given radiant exposure at the catheter tip, the delivered energy per pulse is larger. The theoretical analysis (eq. 2) predicts that this will result in larger vapor bubbles, because the maximal bubble volumes are proportional to the optically active area of the catheter tip. Preliminary experiments with 50–55 mJ/mm<sup>2</sup> excimer laser pulses delivered by 3.5F, 4.0F, 4.5F (normal and multiplexed), and 4.7F multifiber catheters confirm this relation (correlation coefficient of maximal vapor bubble volume vs. optically active area = 0.95) [22,23]. A recent study by Kvasnicka et al. [24] has demonstrated that an increasing ablative surface area of a multifiber catheter, in addition to an increasing ablation efficiency, leads to an increasing extent of adjacent tissue damage. It is tempting to attribute the increased collateral damage to the increased bubble dimensions. On the other hand, decreasing bubble dimension (e.g., by saline flushing or by multiplexing) may decrease the bubble induced mechanical damage and therefore the incidence of dissections [12]. It remains to be established whether the benefit of reduced collateral damage is not offset by reduced contribution of smaller bubbles to the recanalization process.

### Limitations of the Study

In this study, to document the maximal vapor bubbles, time-resolved flash photography was used. Therefore, a non-scattering hemoglobin solution was necessary. Although the hemoglobin solution had a similar hemoglobin concentration and temperature as whole blood, in vivo the results will be different. Furthermore, in our study no tissue boundaries or tissue ablation were applied. Also, clinically used multifiber catheters consist of 20–200 monofibers. The effect of 20–200 small original bubbles uniting in one large vapor bubble will differ from the monofiber used

here. Further investigation on the dynamics of the bubble expansion are needed to address these issues.

### CONCLUSIONS

From this study, we conclude that the previously proposed partial vaporization theory agrees well with the dimensions of experimental excimer laser induced bubbles in hemoglobin for a wide range of conditions. Consequently, both multiplexing the laser pulse and flushing with saline during the laser angioplasty procedure are predicted to decrease the bubble dimensions. It is likely that reduction of the bubble size will lead to reduced mechanical wall damage during pulsed laser angioplasty. Further in vivo and in vitro investigations are needed to confirm this hypothesis.

### ACKNOWLEDGMENTS

We greatly acknowledge Rudolph M. Verdaasdonk of the Laser Center at the Utrecht University Hospital; Geert Gijsbers, Ph.D., and Martin van Gemert, Ph.D., of the Laser Center at the Academic Medical Center in Amsterdam; Masoud Motamedi, Ph.D., of the Biomedical Optics Laboratory, University of Texas, Medical Branch, Galveston, TX; and Steven L. Jacques, Ph.D., at the M.D. Anderson Cancer Center in Houston, TX for their contribution to the article.

The study was supported in part by the Netherlands Heart Foundation (Grant 37.007), by the Albert & Clemmie Caster Foundation, and by the office of Naval Research (Grant N00014-91-J-1564).

### REFERENCES

1. Gijsbers GHM, Sprangers RLH, Keijzer M, de Bakker JMT, van Leeuwen TG, Verdaasdonk RM, Borst C, van Gemert MJC. Some laser-tissue interactions in 308 nm excimer laser coronary angioplasty. *J Interv Cardiol* 1990; 3:231–241.
2. Oraevsky AA, Jacques SL, Pettit GH, Saidi IS, Tittel FK, Henry PD. XeCl laser ablation of atherosclerotic aorta: optical properties and energy pathways. *Lasers Surg Med* 1992; 12:585–597.
3. van Leeuwen TG, Meertens JH, Velema E, Post MJ, Borst C. Intraluminal vapor bubble induced by excimer laser pulse causes microsecond arterial dilation and invagination leading to extensive wall damage in the rabbit. *Circulation* 1993; 87:1258–1263.
4. Anderson RR, Parrish JA. Microvasculature can be selectively damaged using dye lasers: a basic theory and

- experimental evidence in human skin. *Lasers Surg Med* 1981; 1:263–276.
5. Keates RH, Bloom RT, Schneider RT, Ren Q, Sohl J, Viscardi JJ. Absorption of 308-nm excimer laser radiation by balanced salt solution, sodium hyaluronate, and human cadaver eyes. *Arch Ophthalmol* 1990; 108:1611–1613.
  6. Neu W, Nyga R, Tischler C, Haase KK, Karsch KR. Ultrafast imaging of vascular tissue ablation by a XeCl excimer laser. In: Abela GS, Katzir A, eds. "Diagnostic and Therapeutic Cardiovascular Interventions," Vol. 1425 Bellingham, WA: SPIE 1991, pp 37–44.
  7. Preisack MB, Neu W, Nyga R, Wehrmann M, Haase KK, Karsch KR. Ultrafast imaging of tissue ablation by a XeCl excimer laser in saline. *Lasers Surg Med* 1992; 12: 520–527.
  8. Gijsbers GHM, Sprangers RLH, van Gemert MJC. Excimer laser coronary angioplasty: laser-tissue interactions at 308 nm. In: Ginsburg R, Geschwind H, eds. "Primer on Laser Angioplasty." Mount Kisco, NY: Futura Publishing Co., Inc., 1992, pp 217–241.
  9. van Leeuwen TG, van Erven L, Meertens JH, Motamedi M, Post MJ, Borst C. Origin of arterial wall dissections induced by pulsed excimer and mid-infrared laser ablation in the pig. *J Am Coll Cardiol* 1992; 19:1610–1618.
  10. Lane RJ, Wynne JJ, Geronemus RG. Ultraviolet laser ablation of skin: healing studies and a thermal model. *Lasers Surg Med* 1987; 6:504–513.
  11. Litvack F, Eigler NL, Forrester JS. In search of the optimized excimer laser angioplasty system. *Circulation* 1993; 87:1421–1422.
  12. Oberhoff M, Hassenstein S, Hanke H, Xie DY, Blessing E, Baumbach A, Hanke S, Haase KK, Betz E, Karsch KR. Smooth excimer laser coronary angioplasty (SELCA)-initial experimental results [abstract]. *Circulation* 1992; 86(I):800.
  13. van Leeuwen TG, Jansen ED, Motamedi M, Welch AJ, Borst C. Excimer laser ablation of soft tissue: a study of the content of rapidly expanding and collapsing bubbles. *IEEE J Quantum Electron* 1993; 30:1339–1345.
  14. Jansen ED, van Leeuwen TG, Motamedi M, Welch AJ, Borst C. Partial vaporization model for pulsed mid-infrared laser ablation of water. *J Appl Physics* 1995; 75:564–571.
  15. van Leeuwen TG, van der Veen MJ, Verdaasdonk RM, Borst C. Noncontact tissue ablation by holmium:YSGG laser pulses in blood. *Lasers Surg Med* 1991; 11:26–34.
  16. Grigull U, Straub F, Schiebener P. "Steam Tables in SI-Units." Berlin, Germany: Springer-Verlag, 1984.
  17. Lord Rayleigh OM. On the pressure developed in a liquid during the collapse of a spherical cavity. *Phil Mag S* 1917; 34:94–98.
  18. Verdaasdonk RM, Borst C. Ray tracing of optically modified fiber tips 1: spherical probes. *Appl Optics* 1991; 30: 2159–2171.
  19. Yoshikawa M, Nakajima A, Arai T, Kikuchi M, Kannari H, Obara M. Measurement of cavity collapse time by probe technique on water, agar, and vascular tissue during Ho:YAG laser contact ablation. In: Jacques SL, Katzir A, eds. "Laser Tissue Interactions IV," Vol. 1882. Bellingham: SPIE 1993, pp 382–387.
  20. Vogel A, Hentschel W, Holzfuß J, Lauterborn W. Cavi-tation bubble dynamics and acoustic transients generation in ocular surgery with pulsed neodymium:YAG lasers. *Ophthalmology* 1986; 93:1259–1269.
  21. Fischell TA, Stadius ML. New technologies for the treatment of obstructive arterial disease. *Cathet Cardiovasc Diagn* 1991; 22:205–233.
  22. Borst C, van Leeuwen TG. Fundamental laser-tissue interaction: implications for laser coronary angioplasty. [abstract] *Lasers Surg Med* (in press).
  23. van Leeuwen TG, Jansen ED, Welch AJ, Borst C. Reduction of excimer laser-induced vapor bubble size in blood: saline flush and pulse multiplexing. In: Abela GS, Katzir A, eds. "Diagnostic and Therapeutic Cardiovascular Interventions V," Vol 2395C. Bellingham, SPIE 1995, pp 432–440.
  24. Kvasnicka J, Nakamura F, Lange F, Geschwind HJ. Tissue ablation with excimer laser and multiple fiber catheters: effects of optical fiber density and radiant exposures. *J Invertebr Cardiol* 1993; 5:263–273.

## APPENDIX

First, let us consider theoretically, the threshold radiant exposure for bubble formation at the fiber tip submerged in water. Assuming a flat energy profile  $E_{th}$  [mJ] at the fiber tip, the absorbed energy  $dE$  [mJ] in a water layer of an infinitesimal thickness  $dx$  [mm] in front of the fiber tip is given by:

$$dE = \mu_a E_{th} dx \quad (A.1)$$

where  $\mu_a$  is the absorption coefficient of the water [ $\text{mm}^{-1}$ ]. The minimal energy  $dE$  to vaporize the infinitesimal water layer  $dx$  is given by:

$$dE = \rho(c\Delta T + L_v) A dx \quad (A.2)$$

where  $c$  is the specific heat of water [4.2 mJ/mg °C],  $\rho$  is the density of water [1 mg/mm<sup>3</sup>],  $\Delta T$  is the difference between the boiling temperature of water and the ambient water temperature [°C],  $L_v$  the latent heat of vaporization [2,260 mJ/mg] and  $A$  the surface area of the fiber tip [mm<sup>2</sup>]. Neglecting energy losses during the pulse, equating equation 1 and 2 leads to the threshold energy  $E_{th}$  for bubble formation:

$$E_{th} = \rho(c\Delta T + L_v)A/\mu_a \quad (A.3)$$

It follows that the threshold radiant exposure  $H_{th}$  for bubble formation in water, defined as the threshold energy/fiber tip area, is given by:

$$H_{th} = \rho(c\Delta T + L_v)/\mu_a \quad (A.4)$$

Under clinical conditions ( $\Delta T = 100 - 37 = 63^\circ\text{C}$ ) and assuming no heat transfer and a constant absorption coefficient during the pulse, the threshold radiant exposure for bubble formation according to equation A 4 is:



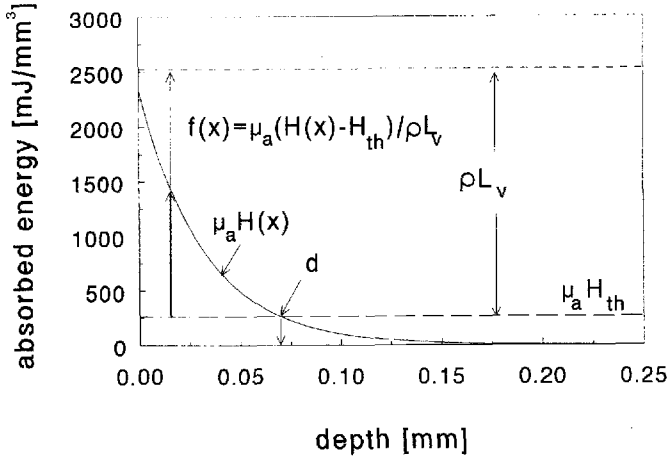


Fig. A.1. The absorbed energy per unit volume for an excimer laser pulse ( $H_0 = 72 \text{ mJ/mm}^2$ ) as a function of depth  $x$  in a hemoglobin solution with  $\mu_a = 32 \text{ mm}^{-1}$ .  $d$  is the depth at which the theoretical threshold radiant exposure for vaporization  $H_{th} = 265/\mu_a \text{ mJ/mm}^2 = 8.2 \text{ mJ/mm}^2$  is reached.  $\rho L_v$  is the latent heat of vaporization.  $f(x)$ , the fraction of the fiber tip area which is vaporized at depth  $x$ , is the ratio of  $\mu_a(H(x) - H_{th})$  and  $\rho L_v$ .

$$H_{th} = 2,525/\mu_a \text{ mJ/mm}^2. \quad (\text{A.5})$$

In most clinical applications of laser tissue interactions, this threshold is considered to be the theoretical threshold radiant exposure for vaporization of tissue water (ablation). However, it has been demonstrated that the threshold radiant exposure for bubble formation is much lower, which was explained by vaporization at a few nucleation sites on the face of the delivery fiber. The area of these nucleation sites,  $A_n$ , is much smaller than the surface area of the fiber tip,  $A$ . Consequently, in our water model, if only a fraction  $f = (A_n/A)$  of the heated water layer area in front of the fiber tip is vaporized, then the threshold radiant exposure for vapor bubble formation is:

$$H_{th} = \rho(c\Delta T + fL_v)/\mu_a. \quad (\text{A.6})$$

If  $f \rightarrow 0$ , then the threshold radiant exposure for bubble formation in water is determined by the radiant exposure sufficient to reach  $100^\circ\text{C}$ . As a result, assuming Beer's law of laser light attenuation in the target liquid and assuming no heat losses and changes in absorption coefficient during the laser pulse, we propose that the (theoretical) threshold radiant exposure for bubble formation is given by:

$$H_{th} = \rho c \Delta T / \mu_a \quad (\text{A.7})$$

resulting in a threshold radiant exposure for water at  $37^\circ\text{C}$  of:

$$H_{th} = 265/\mu_a \text{ mJ/mm}^2. \quad (\text{A.8})$$

Thus, by comparing equations A.5 and A.8, we see that the threshold radiant exposure deduced in equation A.8 is a factor of 9.5 smaller than the theoretically expected threshold as deduced in equation A.5. Note that in clinical practice, the delivered radiant exposure per pulse is 1–10 times the theoretical threshold radiant exposure (eq. A.8) for vaporization of whole blood, assuming  $\mu_a = 32 \text{ mm}^{-1}$  at  $308 \text{ nm}$ . Given the derived threshold radiant exposure  $H_{th}$  (eq. A.7), the maximal amount of water that can be vaporized by a laser pulse with radiant exposure  $H_0$  is to be determined. At the depth  $d$  at which the threshold energy density for bubble formation is reached, the infinitesimally thin layer  $dx$  is heated to  $100^\circ\text{C}$ . Assuming Beer's law:

$$H_{th} = H_0 \exp(-\mu_a d) \quad (\text{A.9})$$

Then  $d$  is given by:

$$d = (1/\mu_a) \ln(H_0/H_{th}) = (1/\mu_a) \ln(E_0/E_{th}) \quad (\text{A.10})$$

with  $E_0$  the pulse energy. Assuming next that the absorbed energy at any depth  $x$  between  $x = 0$  and  $x = d$  is not sufficient to vaporize the whole disc area in front of the fiber, then we assume that the absorbed energy of the laser pulse above threshold ( $E(x) - E_{th}$ ) is the source for partial vaporization of the heated disc at depth  $x$  (Fig. A.1). The fraction  $f(x)$  of the disc at depth  $x$  with area  $A$  that is vaporized is given by:

$$f(x) = (E(x) - E_{th})\mu_a / (\rho A L_v), (f < 1) \quad (\text{A.11})$$

with the energy distribution given by Beer's law:

$$E(x) = E_0 \exp(-\mu_a x). \quad (\text{A.12})$$

Integrating  $f(x) \cdot A$  from  $x = 0$  to  $x = d$  leads to the volume of liquid water beneath the fiber tip which is vaporized:

$$V_{liq} = \int_{x=0}^{x=d} f(x) A dx = \int_{x=0}^{x=d} \frac{\mu_a (E_0 e^{-\mu_a x} - E_{th})}{\rho L_v} dx \quad (\text{A.13})$$

with  $d$  given by eq. A.10. Integration of equation A.13 leads to:

$$V_{liq} = \frac{1}{\rho L_v} \left( E_0 - E_{th} - E_{th} \ln \left( \frac{E_0}{E_{th}} \right) \right) \quad (\text{A.14})$$

which is rewritten to:

$$V_{liq} = \frac{AH_{th}}{\rho L_v} \left( \frac{H_0}{H_{th}} - 1 - \ln \left( \frac{H_0}{H_{th}} \right) \right) \quad (\text{A.15})$$

for  $1 < H_0/H_{th} < 9.5$ .

Note that the restriction  $H_0/H_{th} < 9.5$  is given by the fact that, per definition, the fraction  $f \leq 1$ . From equation A.7 and A.11 and from Figure A.1 it is derived that if the fraction  $f \leq 1$  at the fiber tip ( $x = 0$ ), the ratio  $H_0$  over  $H_{th}$  is given by:

$$H_0/H_{th} \leq (L_v + c\Delta T)/c\Delta T \quad (\text{A.16})$$

Thus, the restriction depends on  $L_v$  (which, e.g., depends on the environmental pressure) and the temperature difference,  $\Delta T$ , between the initial water temperature and the boiling temperature of the water.